Published in final edited form as:
J Immunol. 2010 January 15; 184(2): 931–938. doi:10.4049/jimmunol.0903029.

GRANZYME A AND B-CLUSTER DEFICIENCY DELAYS ACUTE LUNG INJURY IN PNEUMOVIRUS-INFECTED MICE

Reinout A. Bem[*,2], **Job B.M. van Woensel**[*], **Rene Lutter**[‡], **Joseph B. Domachowske**[§], **Jan Paul Medema**[¶], **Helene F. Rosenberg**[#], and **Albert P. Bos**[*]

[*]Pediatric Intensive Care Unit, Emma Children's Hospital AMC, Amsterdam, The Netherlands [‡]Departments of Pulmonology and Experimental Immunology, Academic Medical Center, Amsterdam, The Netherlands [§]Department of Pediatrics, Upstate Medical University, Syracuse, NY, USA [¶]Laboratory for Experimental Oncology and Radiobiology, Academic Medical Center, Amsterdam, The Netherlands [#]Laboratory of Allergic Diseases, National Institute of Allergy and Infectious Diseases, National Institutes of Health, Bethesda, MD, USA

Abstract

Lower respiratory tract infection by the human pneumovirus respiratory syncytial virus is a frequent cause of acute lung injury in children. Severe pneumovirus disease in humans is associated with activation of the granzyme pathway by effector lymphocytes, which may promote pathology by exaggerating pro-apoptotic caspase activity and pro-inflammatory activity. The main goal of this study was to determine whether granzymes contribute to the development of acute lung injury in pneumovirus-infected mice. Granzyme-expressing mice and granzyme A, and B-cluster single and double-gene deleted mice were inoculated with the rodent pneumovirus pneumonia virus of mice strain J3666, and were studied for markers of lung inflammation and injury. Expression of granzyme A and B is detected in effector lymphocytes in mouse lungs in response to pneumovirus infection. Mice deficient for granzyme A and the granzyme B-cluster have unchanged virus titers in the lungs, but show a significantly delayed clinical response to fatal pneumovirus infection, a feature that is associated with delayed neutrophil recruitment, diminished activation of caspase-3 and reduced lung permeability. We conclude that granzyme A and B-cluster deficiency delays the acute progression of pneumovirus disease by reducing alveolar injury.

Keywords

virus; granzyme; apoptosis; lung; lymphocyte

INTRODUCTION

The human pneumovirus, respiratory syncytial virus (RSV)[3], is the leading cause of lower respiratory tract illness in young children and infants worldwide (1). In Western countries the annual incidence rate of RSV-associated hospitalization may be as high as 30 per 1000 children under 1 year of age (1,2). RSV disease in these children presents as bronchiolitis or pneumonia. However, the severe end of the RSV disease spectrum includes the development of acute lung

2**Correspondence**: Reinout A. Bem, Emma Children's Hospital, Academic Medical Center, Pediatric Intensive Care Unit, P.O. Box 22660, 1100 DD, Amsterdam, The Netherlands, Tel: +31 20 5665769, Fax: +31 20 6919338, r.a.bem@amc.uva.nl.

[3]Abbreviations used in this paper: RSV, respiratory syncytial virus; ALI/ARDS, acute lung injury/acute respiratory distress syndrome; PVM, pneumonia virus of mice; Gzm, granzyme; BAL(F), bronchoalveolar lavage (fluid)

injury and acute respiratory distress syndrome (ALI/ARDS), which is characterized by severe hypoxemia and bilateral lung infiltrates in the setting of a normal cardiac preload (3). Currently, treatment for severe RSV disease in normal healthy children is limited to supportive measures, stressing the need to further explore its pathogenesis (4).

In general, ALI/ARDS is associated with the development of diffuse neutrophilic alveolitis and loss of alveolar capillary barrier integrity as a result of enhanced lung epithelial cell death (5). Interestingly, also in humans with severe RSV disease a large number of neutrophils is recruited to the lungs (6), and caspase-dependent apoptosis of lung epithelial cells is observed (7). Similarly, in the pneumonia virus of mice (PVM) mouse model for severe RSV disease (8), pulmonary neutrophil recruitment and caspase-3 activation is associated with enhanced lung permeability and clinical signs of illness (8,9). These findings suggest that the coordinated actions of pro-inflammatory and pro-apoptotic mediators may serve to augment the pathologic responses characteristic of severe pneumovirus disease, although the nature of the mediators linking these responses are not yet fully understood.

Granzymes (Gzms) are effector molecules that may contribute to both inflammatory and apoptotic features of RSV disease. Gzms are serine proteases located in granules of cytotoxic T lymphocytes (CTLs) and natural killer (NK) cells and have traditionally been considered to be crucial to the anti-viral immune response (reviewed in (10–12)). Gzms are delivered into the cytosol of target cells by the pore-forming protein perforin, but intracellular trafficking is also known to be facilitated by adenovirus and bacterial toxins (13,14). Of the five Gzms found in humans (GzmA, B, H, K and M), the tryptase GzmA and aspartase GzmB are the most thoroughly characterized. It has been shown that GzmB induces classical (caspase-dependent) apoptosis in target cells, and *in vitro* micromolar concentrations of GzmA, in the presence of perforin, can induce caspase-independent DNA damage (10,15–17). However, Metkar *et al*. (18) reported recently that GzmA-mediated cytotoxicity at reduced, more physiologic concentrations may be relatively low (15,16). Instead, active soluble GzmA at lower concentrations induces the release of pro-inflammatory cytokines such as IL-1β, IL-6 and TNF-α from monocyte/macrophage, fibroblast and epithelial cell lines via a perforin-independent mechanism (18,19). This raises the possibility that Gzms have a broad functionality in the human immune response to viral infection *in vivo*, including activation of (caspase-dependent) cell death and inflammation.

Recently, our group has demonstrated that tracheal aspirates from mechanically-ventilated children with severe RSV infection contain high levels of biologically active soluble GzmA and GzmB (20). To investigate whether these Gzms may actively participate in the pathogenesis of RSV disease, specifically promoting progression to ALI/ARDS by inducing pro-inflammatory and caspase-dependent pro-apoptotic activity, we explored lung inflammatory and injury markers in acute pneumovirus infection in GzmA and/or GzmB-cluster gene deleted mice.

MATERIAL AND METHODS

Virus and mouse strains

The fully pathogenic PVM strain J3666 was originally obtained from Dr. A.J. Easton (University of Warwick, Coventry, U.K.) from virus stocks originating at the Rockefeller University. Virulence was maintained by continuous passage in mice (21). Virus titer in stock aliquots was 12×10^7 copies of PVM/ml, as determined by quantitative PCR (see below), and PVM inocula per mouse were as indicated.

Nine- to- twelve-week-old female mice were used in all experiments. C57Bl/6 wild type mice ($CD45.1^+$) were originally obtained from Jackson Laboratories (Bar Harbor, ME, USA) and

bred in house. The $GzmA^{-/-}$, $GzmB^{-/-}$ (generated by the group of Dr. T. Ley (22)) and $GzmA^{-/-}GzmB^{-/-}$ mice on a C57Bl/6 background were originally obtained from Dr. M.M. Simon (23) and bred in house (24). $GzmA^{+/-}GzmB^{+/-}$ were used to serve as a primary positive control for the $GzmA^{-/-}GzmB^{-/-}$ mice: $GzmA^{+/-}GzmB^{+/-}$ mice were generated by crossing $GzmA^{-/-}$ with $GzmB^{-/-}$ mice resulting in a similar mixed C57Bl/6 substrain (B6J and B6-III) background as the $GzmA^{-/-}GzmB^{-/-}$ mice (22,25). Importantly, the $GzmB^{-/-}$ (and $GzmA^{-/-}GzmB^{-/-}$) mice lack the entire GzmB-cluster which includes GzmC, -D and -F due to knockdown by a retained phosphoglycerate kinase I gene promoter (PGK-neo) cassette (26).

Animal protocols

The animal protocols as described below were approved by the Animal Care and Experimental Research Committee of the Academic Medical Center Amsterdam, the Netherlands.

PVM diluted in Roswell Park Memorial Institute (RPMI)-medium (Invitrogen Ltd, Paisley, UK) in a total volume of 80μl was delivered via intranasal inhalation to isoflurane anesthetized mice. At day 3, 7 or 8 after inoculation the mice were euthanized with intraperitoneal pentobarbital (120mg/kg), the left lung was removed and flash-frozen in liquid nitrogen for homogenization. Bronchoalveolar lavage (BAL) was performed in the right lung by instilling four separate 0.5 ml aliquots of 0.9% NaCl containing 0.6 mM EDTA. The BAL fluid (BALF) was maintained at 4°C, and spun at 200 *g* for 10 min. The supernatants were stored at −80°C as individual aliquots, and the cell pellet was processed for total cell counts and differentials. For histological analysis on day 8 after PVM inoculation the right lung was fixed with 10% formalin immediately after the BAL procedure.

Measurements

Microarray and flow cytometry analysis—The microarray study as described previously (27), was probed to determine the expression profile of GzmA and GzmB transcripts in whole lung tissue in response to PVM infection. To determine intracellular expression of GzmA and GzmB in effector lymphocytes, BALF leukocytes in FACS buffer (0.5% BSA, 0.02% potassium-EDTA in PBS) were probed with FITC-labeled anti-CD8, PerCP-Cy5-labeled anti-NK1.1 and APC-labeled anti-CD3 (all anti-mouse from eBioscience, San Diego, CA, USA). Next, cells were fixed and permeabilized with fixation/permeabilization solution (BD Biosciences, Franklin Lakes, NJ) and stained with PE-labeled mouse anti-mouse GzmA mAb (Santa Cruz Biotechnology Inc., Heidelberg, Germany) or with PE-labeled rat anti-mouse GzmB mAb (eBioscience) in 10% normal rat serum to block non-specific binding. The FACSCalibur flow cytometer (BD Biosciences) and FlowJo software (Tree Star Inc, Ashland, OR) were used for analysis.

Lung virus titers—Lungs were homogenized in Trizol reagent to extract RNA, according to the manufacturer's description (Invitrogen Ltd., Paisley, UK). RNA was resuspended in DEPC-treated water. After DNaseI treatment of 2 μg RNA (Applied Biosystems, Foster City, CA) cDNA synthesis was performed using a random hexamer cDNA synthesis kit (Applied Biosystems). Copies of the PVM *sh* gene (GenBank: AY573815) were detected in quantitative real-time PCR reactions containing 1 μl cDNA, Taqman PCR Master Mix (Applied Biosystems), 77 nM TAMRA probe (5'-6FAM-CGCTGATAATGGCCTGCAGCA TAMRA-3'), 200 nM primers (5'-GCCTGCATCAACACAGTGTGT-3' and 5'-GCCTGATGTGGCAGTGCTT-3'). The *gapdh* housekeeping gene was detected in cDNA samples using rodent *gapdh* primers (100nM) and VIC-probe (200nM) (Ambion, Applied Biosystems). Standard curves with known concentrations of the full-length *sh*-gene and *gapdh* decatemplate (Applied Biosystems) were used for quantification. Results are expressed as copies of PVM-*sh* per 10^9 copies of *gapdh* (28).

Lung inflammatory markers—Total BALF leukocyte counts were performed on an aliquot of the BALF cells using a Bürker bright line counting chamber. Cytospins were stained with Romanovsky (Diff-Quick) and differential WBC counts were obtained by counting 200 leukocytes using a standard light microscope. Lung cytokines in BALF were measured by multiplex fluorescent bead assay for TNFα, IFNγ, IL-6, IL-1β, KC and MIP-2 (Luminex, R&D systems, Minneapolis, MN).

Lung caspase-activation—Caspase-3 immunohistochemistry on 5-μm-thick paraffin embedded lung sections was performed using rabbit anti-cleaved (active) caspase-3 mAb (Cell Signaling, Danvers, MA) followed by secondary labelling with anti-rabbit IgG HRP polymer (Immunologic, Duiven, The Netherlands). HRP activity was detected with Peroxidase Substrate Kit (Vector®NovaRED, Vector Laboratories, Burlingame, CA). Quantification of the overall lung caspase-3 activity in lung homogenates corrected for lung weight was performed using the caspase-3/CPP32 Fluorometric Assay kit from Biovision, Mountain View (CA) as described previously (29).

Lung permeability—Leakage of the high molecular weight serum protein α-macroglobulin or IgM into the lungs was measured by immunoassay for mouse α-macroglobulin (Life Diagnostics, West Chester, PA) or mouse IgM (Bethyl Laboratories, West Chester, PA) performed on BALF.

Lung histology—A blinded histology analysis for evidence of lung injury was performed on haematoxylin and eosin stained lung sections. A pathological grade for each lung section was determined according to the following criteria: 1 = presence of areas with cellular alveolitis involving 25% or less of the lung parenchyma; 2 = lesions involving 25–50% of the lung; 3 = lesions involving 50% or more of the lung. An additional point was given when there were alveolar wall alterations such as thickening or capillary congestion outside the aforementioned inflammatory areas.

Clinical response—Total body weight and a clinical scoring system previously validated in multiple PVM mouse studies was used: score 1 = healthy, no signs of illness, 2 = subtle ruffled fur, 3 = evident ruffled fur with hunched posture, 4 = evident lethargy with abnormal breathing pattern, 5 = moribund, 6 = death; modified from Cook *et al.* (30)). The endpoint for sacrifice used in this study was a score of 5 and/or loss > 20% of starting body weight.

Statistical analysis

To detect differences among groups we performed either unpaired t-test (for comparison of two groups) or one-way ANOVA (for comparison of multiple groups) followed by LSD post hoc analysis on log10 transformed data. A p value of < 0.05 was considered statistical significant.

RESULTS

Expression of GzmA and GzmB in effector lymphocytes in lungs of PVM-infected mice

Severe pneumovirus (RSV) disease in children is associated with increased local levels of biologically active GzmA and GzmB, and cellular expression of GzmB predominantly in BALF CTLs (20). To determine whether infection with the murine pneumovirus PVM induces GzmA and GzmB expression in mice we analyzed the temporal gene expression profiles of transcripts encoding GzmA and GzmB from a microarray study performed on total lung RNA from C57Bl/6 mice inoculated with a non-lethal dose of PVM (27). Transcripts encoding both GzmA and GzmB were detected in lung tissue from PVM infected mice (Figure 1A). Levels of both the GzmA and GzmB transcript reached a peak at day 7 and remained above baseline

levels until day 14 after inoculation. Immunoreactive GzmA was detected predominantly in $CD3^{-}/NK1.1^{+}$ (NK) cells, and GzmB in $CD8^{+}/CD3^{+}$ (CTL) cells isolated from BALF at day 7 of infection (Figure 1B).

PVM infection in GzmA and GzmB-cluster gene deleted mice

Based on the Gzm gene expression profile, we hypothesized that if the Gzm response contributes either positively or negatively to severe pneumovirus disease, this would become apparent at or beyond peak expression at day 7. To address this question we investigated lung virus titers, caspase-3 activation and cytokine release in wild type, GzmA or GzmB single-gene deleted and GzmAGzmB double-gene deleted mice on day 7 and day 8 after inoculation with PVM (Figure 2).

Surprisingly, whole lung virus titers from PVM-infected wild type mice were indistinguishable from those measured in lungs from PVM-infected $GzmA^{-/-}$, $GzmB^{-/-}$ and $GzmA^{-/-}GzmB^{-/-}$ mice, both on day 7 and 8 after inoculation as determined by quantitative RT-PCR (Figure 2A). However, caspase-3 activity in lung homogenates of the $GzmA^{-/-}GzmB^{-/-}$ mice was significantly reduced compared to the wild type and to the $GzmA^{-/-}$ mice on day 7 and 8 after PVM inoculation (Figure 2B). Previously we have identified that reduced whole lung caspase-3 activity is associated with decreased leakage of the high molecular weight serum protein α-macroglobulin into the alveolar spaces in severe PVM disease in mice (9). In line with this, $GzmB^{-/-}$ and $GzmA^{-/-}GzmB^{-/-}$ mice had reduced concentrations of α-macroglobulin in BALF, as compared to wild type and $GzmA^{-/-}$ mice, although this reached statistical significance only for the $GzmB^{-/-}$ mice (Figure 2C).

PVM infection in mice promotes robust neutrophil influx into the lungs (8). Neutrophil recruitment, as determined by BALF total neutrophil counts, was not different among the wild type, $GzmA^{-/-}$, and $GzmB^{-/-}$ mice; in contrast neutrophil recruitment was delayed in the GzmA and the GzmB-cluster double-gene deleted mice (Figure 2D). However, this delay was not associated with the release of the pro-inflammatory cytokines IL-1β (not detected in any of the mice), IL-6 (Figure 2E) and TNFα (Figure 2F) in the lungs.

PVM infection in $GzmA^{-/-}GzmB^{-/-}$ and $GzmA^{+/-}GzmB^{+/-}$ mice

The findings thus far suggest that Gzms may alter the response to PVM, including caspase-mediated apoptosis and lung permeability, but do not affect viral clearance or the release of the pro-inflammatory cytokines IL-1β, IL-6 and TNFα. We found a more pronounced phenotype in the double-gene deleted mice consistent with previous findings (31). As such, we proceeded with a focus on the $GzmA^{-/-}GzmB^{-/-}$ mice, and to account for the differences in the genetic background of the substrains that may have affected the results above, we compared the lung responses to PVM infection of $GzmA^{-/-}GzmB^{-/-}$ mice to $GzmA^{+/-}GzmB^{+/-}$ mice (22,25).

Viral titers and caspase activation—Consistent with our findings above, whole lung virus titers remained indistinguishable (Figure 3A), while there was a marked reduction in caspase-3 activity in lung homogenates in the $GzmA^{-/-}GzmB^{-/-}$ mice as compared to the $GzmA^{+/-}GzmB^{+/-}$ mice (Figure 3B). To investigate the lung tissue distribution of active caspase-3 in the mice, we performed immunohistochemical localization for cleaved caspase-3 in lung tissue sections of day 8 after PVM inoculation. The lung tissues of $GzmA^{+/-}GzmB^{+/-}$ mice showed widespread cleaved caspase-3 staining in alveolar wall cells and among infiltrating leukocytes (Figure 3C). Interestingly, although PVM replication is detected primarily in bronchial epithelial cells (27), cleaved caspase-3 was not evident in these cells.

Lung permeability—As compared to the $GzmA^{+/-}GzmB^{+/-}$ mice, the $GzmA^{-/-}GzmB^{-/-}$ mice displayed diminished concentrations of α-macroglobulin and IgM in BALF, both markers for lung permeability (9) (Figure 4A and B).

Lung inflammation—As compared to the $GzmA^{+/-}GzmB^{+/-}$ mice, the $GzmA^{-/-}GzmB^{-/-}$ mice had decreased total neutrophil counts in BALF on day 7 after PVM inoculation (Figure 5A). However, this apparent delay in neutrophil influx was not associated with the release of cytokines IL-1β (not detected in any of the mice), IL-6 (Figure 5B), TNFα (Figure 5C), MIP-2 (Figure 5E) or KC (Figure 5F). IFNγ is among the critical regulators of the neutrophil response in PVM infection (32), and was the only cytokine that correlated with the delay in neutrophil recruitment in the $GzmA^{-/-}GzmB^{-/-}$ mice (Figure 5D).

Lung histology—On day 8 after inoculation with PVM, the lung tissues from all mice showed extensive peri-bronchial and peri-vascular cellular infiltrates, as well as areas with acute alveolitis and alveolar wall alterations such as thickening and (mild hemorrhagic) capillary congestion, similar to findings described previously (8). However, cellular alveolitis and capillary congestion was more diffuse in the $GzmA^{+/-}GzmB^{+/-}$ mice, when compared to $GzmA^{-/-}GzmB^{-/-}$ mice (Figure 6): mean (± SE) histopathology scores were 3.2 (0.3) in the $GzmA^{-/+}GzmB^{-/+}$ mice, and 2.2 (0.2) in the $GzmA^{-/-}GzmB^{-/-}$ mice ($p<0.05$).

Clinical response—Finally, to address whether these Gzm-mediated alterations of the lung response to PVM affect the clinical phenotype, we followed clinical scores and body weight up to day 12 after inoculation with a lethal inoculum of PVM. The $GzmA^{-/-}GzmB^{-/-}$ mice showed a statistically significant delay in reaching the maximum clinical response to PVM (Figure 7A). All the $GzmA^{+/-}GzmB^{+/-}$ mice reached the defined endpoint (clinical score of 5 and/or body weight loss > 20%) at day 10 after PVM inoculation, whereas at this point this was reached by 67% of the $GzmA^{-/-}GzmB^{-/-}$ mice ($p<0.05$). A delayed response to PVM infection among the $GzmA^{-/-}GzmB^{-/-}$ mice was also observed when weight loss alone as a sole, purely objective measure of the clinical response was examined (Figure 7B).

DISCUSSION

The primary goal of this study was to determine whether Gzms promote pathophysiologic responses, including acute lung injury, in pneumovirus-infected mice. In this work, we detect both GzmA (predominantly in NK cells) and GzmB (predominantly in CTLs) in association with severe respiratory sequelae induced by the mouse pneumovirus pathogen, PVM. We found that mice deficient for both GzmA and the GzmB-cluster ($GzmA^{-/-}GzmB^{-/-}$) have a delayed clinical response to fatal PVM infection, although Gzm expression has no impact on virus replication or clearance per se. Instead, we determine that the absence of Gzms results in delayed neutrophil recruitment, diminished activation of caspase-3 and reduced lung permeability.

The Gzm system exploited by effector lymphocytes plays a major role in host anti-viral immunity by activating cell death programs in infected target cells (10–12). Providing the first *in vivo* evidence for Gzm-mediated viral elimination, Mullbacher *et al*. (31) showed that the survival and clearance of the mouse poxvirus, ectromelia, in mice lacking both GzmA and the GzmB-cluster was markedly depressed as compared to wild type mice. Systematic challenge of Gzm-deficient mice to different virus families has not been undertaken, but replication of cytomegalovirus and herpes simplex virus have also found to be controlled by Gzm activity (33,34). At the same time, there is much evidence that effector lymphocyte-mediated immunopathogenic mechanisms form the basis of enhanced disease in certain virus infections, and this includes the development of severe human pneumovirus (RSV) disease (35,36). For example, both CTLs and NK cells are recruited to the lungs during primary RSV infection in

mice (36–38). Depletion of CTLs in mice reduces clinical signs of RSV disease, despite delaying viral clearance (36), while intravenous transfer of high dose CTLs into CTL-depleted mice causes severe hemorrhage and neutrophilic inflammation (39). Frey *et al*. (40) studied the PVM mouse model, which, unlike RSV infection in mice, reproduces several features of *severe* RSV disease in humans, including robust viral replication, pro-inflammatory alterations in the airways and alveoli, alveolar injury and importantly, overt clinical signs of illness (8). They found similar results, namely, that T-cell deficient mice have a delayed clearance of PVM, but reduced pulmonary inflammatory infiltrates and weight loss (40). These findings suggested that effector lymphocytes may contribute to the immunopathophysiology associated with human RSV infection, but whether the Gzm system is involved herein remained unclear from those studies.

Recently, we found high levels of active GzmA and GzmB in tracheal aspirates from children with severe RSV disease (20). Surprisingly, in the present study, virus titers in lung tissue were not altered by Gzm-targeting, despite a major reduction in lung caspase-3 activation in GzmA and GzmB-cluster deficient mice. Similarly, Frey *et al*. (40) found that mice deficient for perforin, which facilitates granzyme-trafficking into virus-infected target cells, did not alter PVM lung titers. These findings suggest that alternative pathways may play more prominent roles in PVM clearance. Certain viruses, such as adenovirus and parainfluenza virus type 3, are known to have evolved strategies that specifically inhibit GzmB (41,42), and poxvirus can block caspase signaling (11,43). Interestingly, in our study we found little to no caspase-3 activation in bronchial epithelial cells, clearly the most important site for PVM replication (27). However it is currently unknown whether PVM directly induces anti-apoptotic pathways in infected bronchial epithelial cells.

Similar to previous findings (9), PVM infection was associated with increased caspase-3 activation in alveolar wall cells, and this was markedly reduced in Gzm-deficient mice. As such, this finding may explain at least in part the observed decreased lung permeability in the Gzm-deficient mice. Accumulating evidence implicates caspase-dependent apoptosis as an important mechanism leading to loss of alveolar capillary barrier integrity and ultimately enhanced lung permeability (44). Patients who die with ALI/ARDS have increased caspase-3 staining in alveolar wall cells (45), and numerous experimental studies modelling both indirect and direct ALI/ARDS have shown enhanced apoptosis of lung epithelial cells is associated with leakage of serum proteins into the lungs and histopathological alterations, which can be attenuated by inhibiting pro-apoptotic pathways (44,46,47). Our findings suggest the Gzm pro-apoptotic pathway can contribute to the development of alveolar injury in severe pneumovirus disease. Interestingly, both GzmA and GzmB mRNA expression is augmented in patients with septic ARDS and in mice intratracheally instilled with LPS (47,48), suggesting the Gzm pathway may also be of relevance to bacterial-induced ALI/ARDS .

In addition to pro-apoptotic functions of Gzms, recent renewed attention has been given to their potential pro-inflammatory effects, specifically of GzmA (18,19). Metkar *et al*. (18) found that active human GzmA induces the release of IL-1β, IL-6 and TNF-α from monocytes, which can be attenuated by the IL-1β convertase (caspase-1) inhibitor WEHD-FMK, and similarly, that mouse macrophages produce IL-1β in response to treatment with active mouse GzmA. Interestingly, GzmA and GzmB-cluster deficient mice showed a delayed lung neutrophil response to PVM infection, but this was not associated with the release of IL-1β, IL-6, TNF-α, KC and MIP-2. The fact that we did not detect IL-1β in the BALF of any of the mice may suggest that the above mentioned mechanism of GzmA-mediated pro-inflammatory activity through caspase-1 may not be directly relevant in the PVM natural infection model. IFNγ, potentially released from activated NK cells, has been identified as a critical regulator of neutrophil influx into the lungs in severe PVM disease in mice (32), and followed the same pattern as the total neutrophil counts in the GzmA and GzmB-cluster deficient mice. However,

it remains to be elucidated whether mouse Gzm may directly mediate the release of IFNγ, as for example, human GzmA does not induce IFNγ specifically in monocytes (18). In addition, one needs to recognize that a number of different events, including adhesion, migration and clearance, affect the number of neutrophils in the lungs. In this light, the potent proteolytic degradation of extracellular matrix proteins by both GzmA and GzmB is of particular interest, because Gzm-mediated remodelling of the extracellular environment has been shown to have important consequences for cellular migration and survival (49).

As stated above, in the most current paradigm, GzmA elicits predominantly pro-inflammatory activity, while GzmB mediates caspase-dependent apoptosis, based mostly on observations *in vitro* (15,16). However, deciphering the specific functions of the individual Gzm family members *in vivo* has proven to be difficult and not straightforward (11,16,18,31). Interestingly, studies in mice have shown that the combined deficiency for GzmA and the GzmB-cluster can result in a more pronounced or paradoxically diminished phenotype, as compared to single-gene (GzmA or the GzmB-cluster) deficiency (18,31), suggesting complex and synergistic interaction between Gzms. The interpretation of experiments involving Gzm targeted mice is further complicated by the fact that the GzmB-gene deleted mice lack the entire GzmB-cluster which includes GzmC, -D and -F (26). In addition, the differences in substrain background between wild type, single-gene and double-gene Gzm deleted mice may affect host responses to pathogens. Finally, *in vivo*, through indirect mechanisms involving inflammatory cells and extra-cellular matrix remodeling, Gzms may influence several processes, including cell death pathways (49), to which they are not directly attributed to: e.g. while GzmA does not directly cause caspase activation, in our study, GzmA single-gene deleted mice showed some reduction in lung caspase-3 activity. Taking into account these several issues, we have primarily focused on the effects of combined deficiency for GzmA and the GzmB-cluster, but this obviously limits our interpretation of the functions of the individual Gzm family members in acute pneumovirus infection.

Finally, it is important to recognize that mouse and human Gzm differ in structure, enzyme activity and inhibitory regulation (50). For example, human GzmB is more cytotoxic than mouse GzmB *in vitro* (50). In addition, unlike mouse GzmB, the human form requires Bid cleavage for full caspase-3 activation, and is controlled by the inhibitor PI-9 (50). Furthermore, the evolution of the Gzm system, potentially driven by host specific pathogens, may compromise some of the meaning of any study of Gzm responses to human virus pathogens inoculated in mice. As such, the use of the natural mouse pneumovirus pathogen, PVM, in this work may represent an important advantage, as it permits us to explore the roles and functions of Gzms in response to a physiologically and evolutionarily relevant challenge. On the other hand, although PVM and RSV are both pneumoviruses, they are not the same virus, and we need to stress there is no one animal model that displays all features of human RSV disease.

In conclusion, pneumovirus infection in mice induces expression of GzmA and GzmB by effector lymphocytes. The combined deficiency of GzmA and the GzmB-cluster results in a delayed progression of pneumovirus disease by reducing alveolar injury in mice, without altering viral clearance. We speculate that targeting of the Gzm system in humans may be beneficial in diminishing RSV-ALI/ARDS immunopathogenesis.

Acknowledgments

The authors thank P.J. van de Berg for expert advice on FACS analysis, and J. de Jong for assistance with animal breeding.

Gants/funding: supported in part by Ars Donandi, Amsterdam. H.F. Rosenberg supported by National Institute of Allergy and Infectious Diseases Division of Intramural Research (Z01-AI000943).

REFERENCES

1. Hall CB, Weinberg GA, Iwane MK, Blumkin AK, Edwards KM, Staat MA, Auinger P, Griffin MR, Poehling KA, Erdman D, Grijalva CG, Zhu Y, Szilagyi P. The burden of respiratory syncytial virus infection in young children. N. Engl. J. Med 2009;360:588–598. [PubMed: 19196675]
2. Shay DK, Holman RC, Newman RD, Liu LL, Stout JW, Anderson LJ. Bronchiolitis-associated hospitalizations among US children, 1980–1996. JAMA 1999;282:1440–1446. [PubMed: 10535434]
3. Dahlem P, van Aalderen WM, Hamaker ME, Dijkgraaf MG, Bos AP. Incidence and short-term outcome of acute lung injury in mechanically ventilated children. Eur. Respir. J 2003;22:980–985. [PubMed: 14680089]
4. Nokes JD, Cane PA. New strategies for control of respiratory syncytial virus infection. Curr. Opin. Infect. Dis 2008;21:639–643. [PubMed: 18978532]
5. Ware LB, Matthay MA. The acute respiratory distress syndrome. N. Engl. J Med 2000;342:1334–1349. [PubMed: 10793167]
6. Wang SZ, Forsyth KD. The interaction of neutrophils with respiratory epithelial cells in viral infection. Respirology 2000;5:1–10. [PubMed: 10728725]
7. Welliver TP, Reed JL, Welliver RC Sr. Respiratory syncytial virus and influenza virus infections: observations from tissues of fatal infant cases. Pediatr. Infect. Dis. J 2008;27:S92–S96. [PubMed: 18820587]
8. Rosenberg HF, Domachowske JB. Pneumonia virus of mice: severe respiratory infection in a natural host. Immunol. Lett 2008;118:6–12. [PubMed: 18471897]
9. Bem RA, van Woensel JB, Bos AP, Koski A, Farnand AW, Domachowske JB, Rosenberg HF, Martin TR, Matute-Bello G. Mechanical ventilation enhances lung inflammation and caspase activity in a model of mouse pneumovirus infection. Am. J Physiol Lung Cell Mol. Physiol 2009;296:L46–L56. [PubMed: 18996903]
10. Lieberman J. The ABCs of granule-mediated cytotoxicity: new weapons in the arsenal. Nat. Rev. Immunol 2003;3:361–370. [PubMed: 12766758]
11. Russell JH, Ley TJ. Lymphocyte-mediated cytotoxicity. Annu. Rev. Immunol 2002;20:323–370. [PubMed: 11861606]
12. Bots M, Medema JP. Granzymes at a glance. J Cell Sci 2006;119:5011–5014. [PubMed: 17158907]
13. Browne KA, Blink E, Sutton VR, Froelich CJ, Jans DA, Trapani JA. Cytosolic delivery of granzyme B by bacterial toxins: evidence that endosomal disruption, in addition to transmembrane pore formation, is an important function of perforin. Mol. Cell Biol 1999;19:8604–8615. [PubMed: 10567584]
14. Froelich CJ, Orth K, Turbov J, Seth P, Gottlieb R, Babior B, Shah GM, Bleackley RC, Dixit VM, Hanna W. New paradigm for lymphocyte granule-mediated cytotoxicity. Target cells bind and internalize granzyme B, but an endosomolytic agent is necessary for cytosolic delivery and subsequent apoptosis. J. Biol. Chem 1996;271:29073–29079. [PubMed: 8910561]
15. Froelich CJ, Pardo J, Simon MM. Granule-associated serine proteases: granzymes might not just be killer proteases. Trends Immunol 2009;30:117–123. [PubMed: 19217825]
16. Trapani JA, Bird PI. A renaissance in understanding the multiple and diverse functions of granzymes? Immunity 2008;29:665–667. [PubMed: 19006688]
17. Martinvalet D, Dykxhoorn DM, Ferrini R, Lieberman J. Granzyme A cleaves a mitochondrial complex I protein to initiate caspase-independent cell death. Cell 2008;133:681–692. [PubMed: 18485875]
18. Metkar SS, Menaa C, Pardo J, Wang B, Wallich R, Freudenberg M, Kim S, Raja SM, Shi L, Simon MM, Froelich CJ. Human and mouse granzyme A induce a proinflammatory cytokine response. Immunity 2008;29:720–733. [PubMed: 18951048]
19. Sower LE, Klimpel GR, Hanna W, Froelich CJ. Extracellular activities of human granzymes. I. Granzyme A induces IL6 and IL8 production in fibroblast and epithelial cell lines. Cell Immunol 1996;171:159–163.
20. Bem RA, Bos AP, Bots M, Wolbink AM, van Ham SM, Medema JP, Lutter R, van Woensel JB. Activation of the granzyme pathway in children with severe respiratory syncytial virus infection. Pediatr Res 2008;63:650–655. [PubMed: 18317234]

21. Domachowske JB, Bonville CA, Gao JL, Murphy PM, Easton AJ, Rosenberg HF. The chemokine macrophage-inflammatory protein-1 alpha and its receptor CCR1 control pulmonary inflammation and antiviral host defense in paramyxovirus infection. J Immunol 2000;165:2677–2682. [PubMed: 10946298]
22. Heusel JW, Wesselschmidt RL, Shresta S, Russell JH, Ley TJ. Cytotoxic lymphocytes require granzyme B for the rapid induction of DNA fragmentation and apoptosis in allogeneic target cells. Cell 1994;76:977–987. [PubMed: 8137431]
23. Simon MM, Hausmann M, Tran T, Ebnet K, Tschopp J, ThaHla R, Mullbacher A. In vitro- and ex vivo-derived cytolytic leukocytes from granzyme A × B double knockout mice are defective in granule-mediated apoptosis but not lysis of target cells. J Exp. Med 1997;186:1781–1786. [PubMed: 9362539]
24. Bots M, Kolfschoten IG, Bres SA, Rademaker MT, de Roo GM, Kruse M, Franken KL, Hahne M, Froelich CJ, Melief CJ, Offringa R, Medema JP. SPI-CI and SPI-6 cooperate in the protection from effector cell-mediated cytotoxicity. Blood 2005;105:1153–1161. [PubMed: 15454490]
25. Ebnet K, Hausmann M, Lehmann-Grube F, Mullbacher A, Kopf M, Lamers M, Simon MM. Granzyme A-deficient mice retain potent cell-mediated cytotoxicity. EMBO J 1995;14:4230–4239. [PubMed: 7556064]
26. Revell PA, Grossman WJ, Thomas DA, Cao X, Behl R, Ratner JA, Lu ZH, Ley TJ. Granzyme B and the downstream granzymes C and/or F are important for cytotoxic lymphocyte functions. J. Immunol 2005;174:2124–2131. [PubMed: 15699143]
27. Bonville CA, Bennett NJ, Koehnlein M, Haines DM, Ellis JA, DelVecchio AM, Rosenberg HF, Domachowske JB. Respiratory dysfunction and proinflammatory chemokines in the pneumonia virus of mice (PVM) model of viral bronchiolitis. Virology 2006;349:87–95. [PubMed: 16563455]
28. Ellis JA, Martin BV, Waldner C, Dyer KD, Domachowske JB, Rosenberg HF. Mucosal inoculation with an attenuated mouse pneumovirus strain protects against virulent challenge in wild type and interferon-gamma receptor deficient mice. Vaccine 2007;25:1085–1095. [PubMed: 17052820]
29. Bem RA, Farnand AW, Wong V, Koski A, Rosenfeld ME, van RN, Frevert CW, Martin TR, Matute-Bello G. Depletion of resident alveolar macrophages does not prevent Fas-mediated lung injury in mice. Am. J Physiol Lung Cell Mol. Physiol 2008;295:L314–L325. [PubMed: 18556802]
30. Cook PM, Eglin RP, Easton AJ. Pathogenesis of pneumovirus infections in mice: detection of pneumonia virus of mice and human respiratory syncytial virus mRNA in lungs of infected mice by in situ hybridization. J Gen. Virol 1998;79(Pt 10):2411–2417. [PubMed: 9780046]
31. Mullbacher A, Waring P, Tha HR, Tran T, Chin S, Stehle T, Museteanu C, Simon MM. Granzymes are the essential downstream effector molecules for the control of primary virus infections by cytolytic leukocytes. Proc. Natl. Acad. Sci U. S. A 1999;96:13950–13955. [PubMed: 10570179]
32. Bonville CA, Percopo CM, Dyer KD, Gao J, Prussin C, Foster B, Rosenberg HF, Domachowske JB. Interferon-gamma coordinates CCL3-mediated neutrophil recruitment in vivo. BMC. Immunol 2009;10:14. [PubMed: 19298652]
33. Pereira RA, Simon MM, Simmons A. Granzyme A, a noncytolytic component of CD8(+) cell granules, restricts the spread of herpes simplex virus in the peripheral nervous systems of experimentally infected mice. J Virol 2000;74:1029–1032. [PubMed: 10623769]
34. Riera L, Gariglio M, Valente G, Mullbacher A, Museteanu C, Landolfo S, Simon MM. Murine cytomegalovirus replication in salivary glands is controlled by both perforin and granzymes during acute infection. Eur. J Immunol 2000;30:1350–1355. [PubMed: 10820381]
35. Domachowske JB, Rosenberg HF. Respiratory syncytial virus infection: immune response, immunopathogenesis, and treatment. Clin. Microbiol. Rev 1999;12:298–309. [PubMed: 10194461]
36. Graham BS, Bunton LA, Wright PF, Karzon DT. Role of T lymphocyte subsets in the pathogenesis of primary infection and rechallenge with respiratory syncytial virus in mice. J Clin. Invest 1991;88:1026–1033. [PubMed: 1909350]
37. Hussell T, Openshaw PJ. Intracellular IFN-gamma expression in natural killer cells precedes lung CD8+ T cell recruitment during respiratory syncytial virus infection. J. Gen. Virol 1998;79(Pt 11): 2593–2601. [PubMed: 9820134]
38. Openshaw PJ. Flow cytometric analysis of pulmonary lymphocytes from mice infected with respiratory syncytial virus. Clin. Exp. Immunol 1989;75:324–328. [PubMed: 2784741]

39. Cannon MJ, Openshaw PJ, Askonas BA. Cytotoxic T cells clear virus but augment lung pathology in mice infected with respiratory syncytial virus. J Exp. Med 1988;168:1163–1168. [PubMed: 3262705]
40. Frey S, Krempl CD, Schmitt-Graff A, Ehl S. Role of T cells in virus control and disease after infection with pneumonia virus of mice. J. Virol 2008;82:11619–11627. [PubMed: 18815308]
41. Andrade F, Bull HG, Thornberry NA, Ketner GW, Casciola-Rosen LA, Rosen A. Adenovirus L4-100K assembly protein is a granzyme B substrate that potently inhibits granzyme B-mediated cell death. Immunity 2001;14:751–761. [PubMed: 11420045]
42. Sieg S, Xia L, Huang Y, Kaplan D. Specific inhibition of granzyme B by parainfluenza virus type 3. J. Virol 1995;69:3538–3541. [PubMed: 7745701]
43. Zhou Q, Snipas S, Orth K, Muzio M, Dixit VM, Salvesen GS. Target protease specificity of the viral serpin CrmA. Analysis of five caspases. J. Biol. Chem 1997;272:7797–7800. [PubMed: 9065443]
44. Martin TR, Hagimoto N, Nakamura M, Matute-Bello G. Apoptosis and epithelial injury in the lungs. Proc. Am. Thorac. Soc 2005;2:214–220. [PubMed: 16222040]
45. Albertine KH, Soulier MF, Wang Z, Ishizaka A, Hashimoto S, Zimmerman GA, Matthay MA, Ware LB. Fas and fas ligand are up-regulated in pulmonary edema fluid and lung tissue of patients with acute lung injury and the acute respiratory distress syndrome. Am. J. Pathol 2002;161:1783–1796. [PubMed: 12414525]
46. Kawasaki M, Kuwano K, Hagimoto N, Matsuba T, Kunitake R, Tanaka T, Maeyama T, Hara N. Protection from lethal apoptosis in lipopolysaccharide-induced acute lung injury in mice by a caspase inhibitor. Am. J. Pathol 2000;157:597–603. [PubMed: 10934162]
47. Kitamura Y, Hashimoto S, Mizuta N, Kobayashi A, Kooguchi K, Fujiwara I, Nakajima H. Fas/FasL-dependent apoptosis of alveolar cells after lipopolysaccharide-induced lung injury in mice. Am. J. Respir. Crit Care Med 2001;163:762–769. [PubMed: 11254536]
48. Hashimoto S, Kobayashi A, Kooguchi K, Kitamura Y, Onodera H, Nakajima H. Upregulation of two death pathways of perforin/granzyme and FasL/Fas in septic acute respiratory distress syndrome. Am. J. Respir. Crit Care Med 2000;161:237–243. [PubMed: 10619826]
49. Buzza MS, Bird PI. Extracellular granzymes: current perspectives. Biol. Chem 2006;387:827–837. [PubMed: 16913832]
50. Kaiserman D, Bird CH, Sun J, Matthews A, Ung K, Whisstock JC, Thompson PE, Trapani JA, Bird PI. The major human and mouse granzymes are structurally and functionally divergent. J Cell Biol 2006;175:619–630. [PubMed: 17116752]

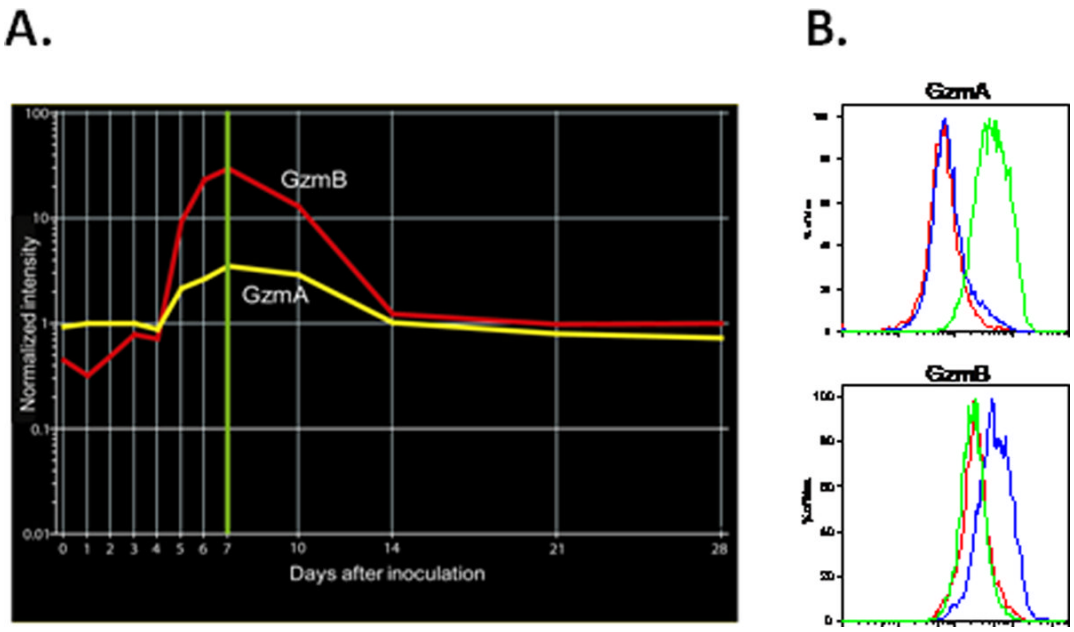

Figure 1.

PVM infection induces expression of GzmA and GzmB. *A*, gene expression profiles of transcripts encoding GzmA and GzmB in total lung RNA of C57Bl/6 mice (RNA from 5 mice pooled per time point) at time zero and days 1–7, 10, 14, 21 and 28 after inoculation with PVM J3666 (30 pfu). Peak of GzmA and GzmB expression at day 7 (green highlight). *B*, histogram plots of intracellular GzmA and GzmB expression in BALF $CD8^{+}CD3^{+}$ cells (CTLs, blue plot), $NK1.1^{+}CD3^{-}$ (NK cells, green plot) and $CD8^{-}CD3^{+}$ ($CD8^{-}$ T lymphocytes, red plot) of PVM-infected mice at day 7 (BALF leukocytes from 3 mice pooled).

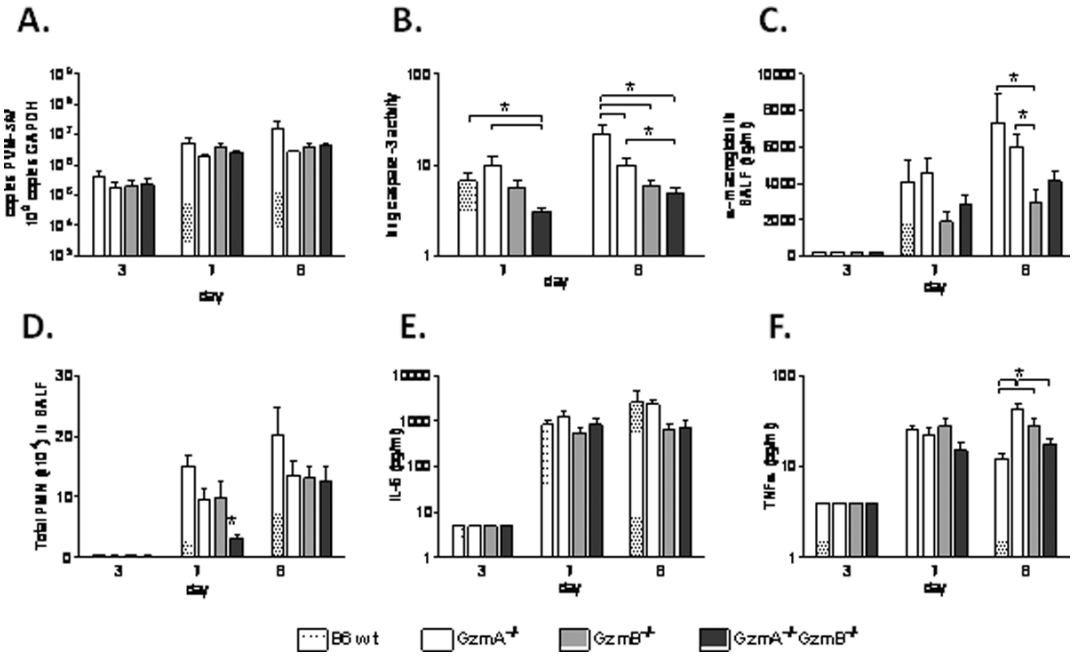

Figure 2.

Lung response to PVM infection in GzmA and GzmB-cluster gene deleted mice. *A*, virus titer in the lung, expressed as number of PVM-*sh* copies per 10^9 *gapdh* copies; *B*, lung homogenate caspase-3 activity (arbitrary fluorescence units); *C*, concentration of α-macroglobulin in BALF; *D*, BALF total neutrophil (PMN) counts; *E*, concentration of IL-6 (pg/ml) in BALF; and *F*, concentration of TNFα (pg/ml) in BALF, in the wild type (B6 wt), $GzmA^{-/-}$, $GzmB^{-/-}$ and $GzmA^{-/-}GzmB^{-/-}$ mice on day 3 (n=3 per group), 7 (n=6 per group) and 8 (n=4–6 per group) after PVM inoculation (6×10^3 copies). * $p<0.05$. Data are shown as bar graphs depicting mean and standard error.

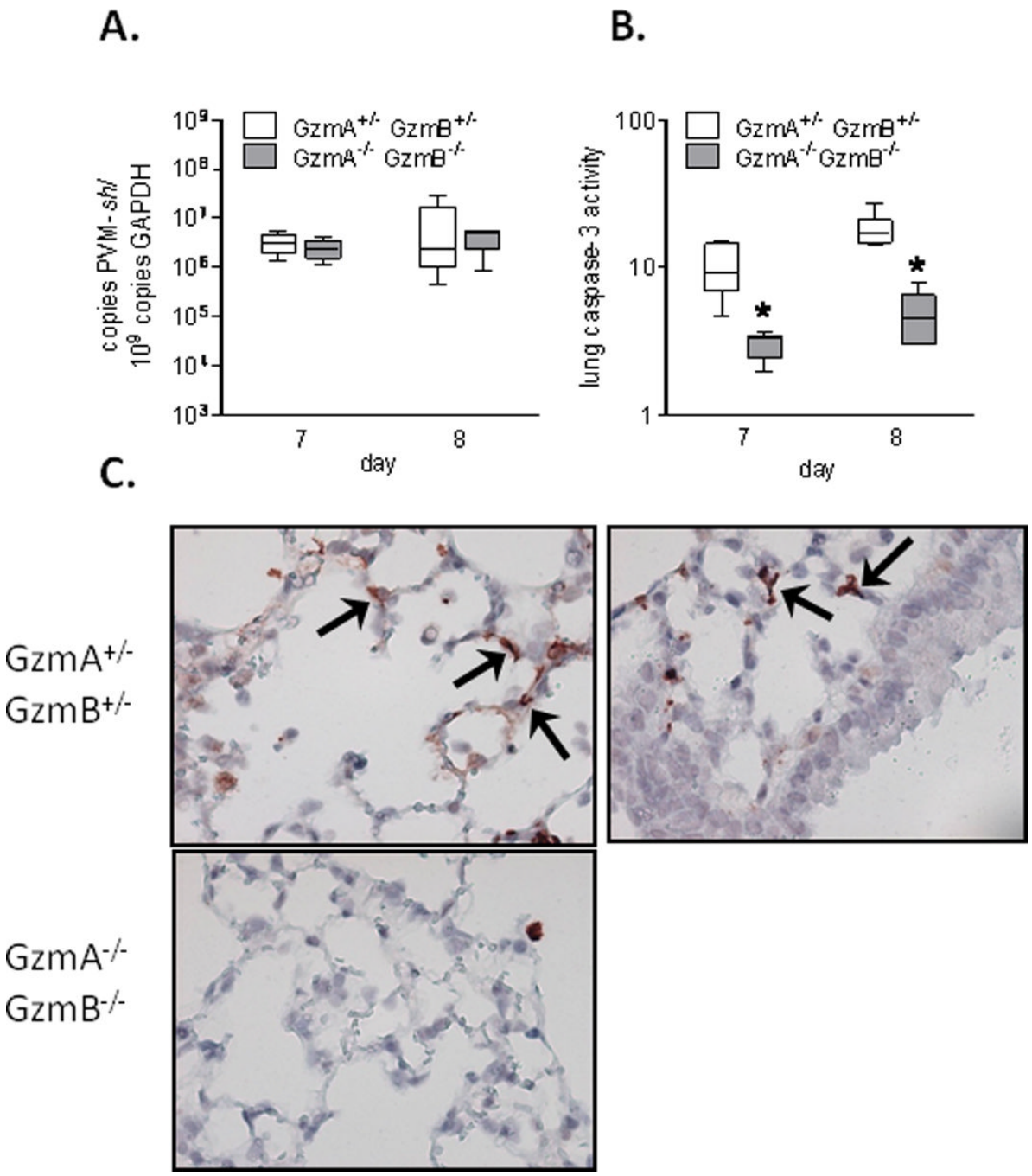

Figure 3.

PVM clearance and apoptosis in GzmA and GzmB-cluster gene deleted mice. *A*, virus titer in the lung, expressed as number of PVM-*sh* copies per 10^9 *gapdh* copies; *B*, lung homogenate caspase-3 activity (arbitrary fluorescence units), in the $GzmA^{+/-}GzmB^{+/-}$ mice and $GzmA^{-/-}GzmB^{-/-}$ mice on day 7 (n=6 per group) and 8 (n=6 per group) after PVM inoculation (6×10^3 copies). * $p<0.05$. Data are shown as box plots depicting the median, interquartile range and full range. *C*, representative images of cleaved caspase-3 immunohistochemistry in lung tissues of the $GzmA^{+/-}GzmB^{+/-}$ mice and $GzmA^{-/-}GzmB^{-/-}$ mice on day 8 after PVM inoculation. Note the relative positive staining in alveolar wall cells (arrows) as compared to bronchial epithelial cells in the $GzmA^{+/-}GzmB^{+/-}$ mice.

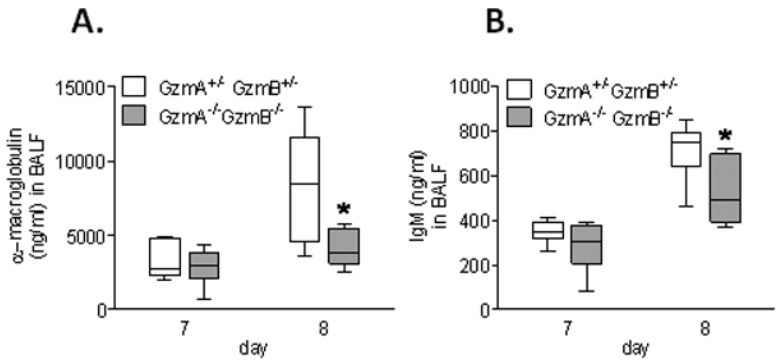

Figure 4.

Lung permeability response to PVM infection in GzmA and GzmB-cluster gene deleted mice. Concentration of α-macroglobulin (*A*) and IgM (*B*) in BALF of the $GzmA^{+/-}GzmB^{+/-}$ mice and $GzmA^{-/-}GzmB^{-/-}$ mice on day 7 (n=6 per group) and 8 (n=6 per group) after PVM inoculation (6×10^3 copies). * $p<0.05$. Data are shown as box plots depicting the median, interquartile range and full range.

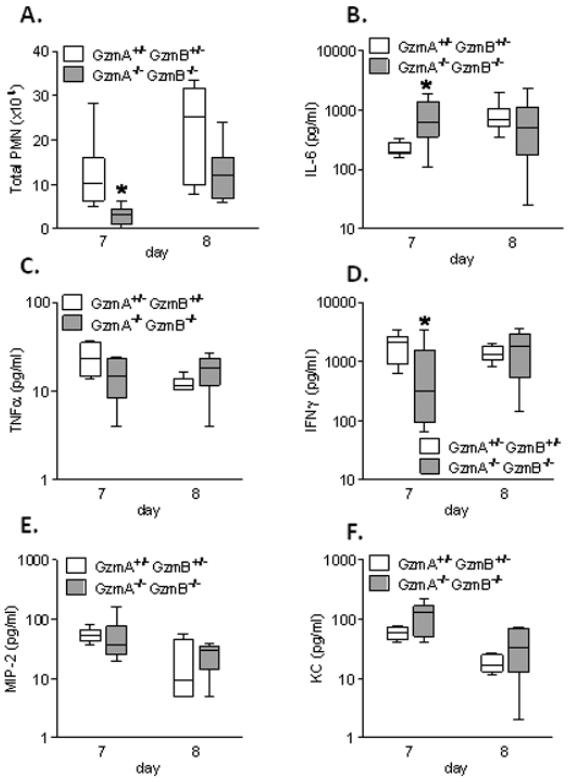

Figure 5.

Lung inflammatory response to PVM infection in GzmA and GzmB-cluster gene deleted mice. Total neutrophil (PMN) counts (*A*), and concentrations of IL-6 (*B*), TNFα (*C*), IFNγ (*D*), MIP-2 (*E*) and KC (*F*) in BALF of the $GzmA^{+/-}GzmB^{+/-}$ mice and $GzmA^{-/-}GzmB^{-/-}$ mice on day 7 (n=6 per group) and 8 (n=6 per group) after PVM inoculation (6×10^3 copies). * $p<0.05$. Data are shown as box plots depicting the median, interquartile range and full range.

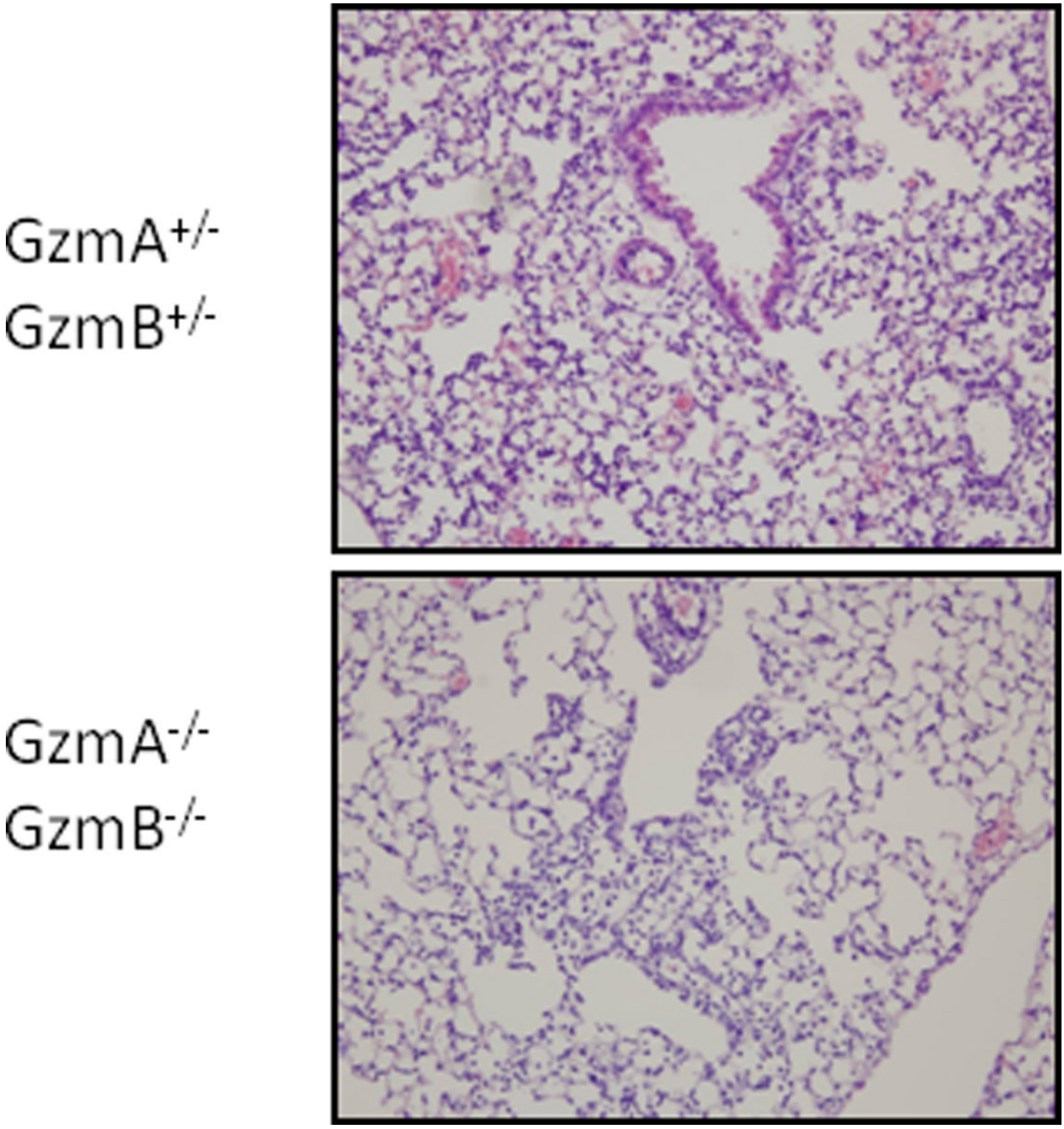

Figure 6.
Lung tissue response to PVM infection in GzmA and GzmB-cluster gene deleted mice. Representative images of haematoxylin and eosin stained lung tissue from the $GzmA^{+/-}GzmB^{+/-}$ mice and $GzmA^{-/-}GzmB^{-/-}$ mice on day 8 after PVM inoculation (6×10^3 copies). Magnification 100x.

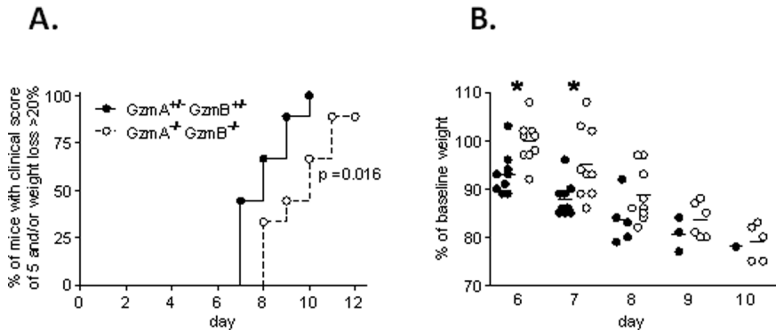

Figure 7.

Clinical response to PVM infection in GzmA and GzmB-cluster gene deleted mice. *A*, Kaplan-Meier curves showing the percentages of $GzmA^{+/-}GzmB^{+/-}$ (black dots, n=9) and $GzmA^{-/-}GzmB^{-/-}$ (white dots, n=9) mice reaching the endpoint of a clinical score of 5 (moribund) and/or weight loss > 20% after PVM inoculation (1×10^4 copies). $p < 0.05$ by log-rank (Mantel-Cox) test. *B*, percentage of baseline (day 0) weight of the $GzmA^{+/-}GzmB^{+/-}$ (black dots) and $GzmA^{-/-}GzmB^{-/-}$ (white dots) mice after PVM inoculation (1×10^4 copies). * $p < 0.05$. Bars show the mean.